



**HAL**  
open science

# Global 4DVAR Assimilation and Forecast Experiments Using AMSU Observations over Land. Part I: Impacts of Various Land Surface Emissivity Parameterizations

Fatima Karbou, Florence Rabier, Elisabeth Gerard

► **To cite this version:**

Fatima Karbou, Florence Rabier, Elisabeth Gerard. Global 4DVAR Assimilation and Forecast Experiments Using AMSU Observations over Land. Part I: Impacts of Various Land Surface Emissivity Parameterizations. *Weather and Forecasting*, 2009, pp.PP. 5-19. 10.1175/2009WAF2222243.1 . meteo-00463475

**HAL Id: meteo-00463475**

**<https://meteofrance.hal.science/meteo-00463475>**

Submitted on 22 Oct 2021

**HAL** is a multi-disciplinary open access archive for the deposit and dissemination of scientific research documents, whether they are published or not. The documents may come from teaching and research institutions in France or abroad, or from public or private research centers.

L'archive ouverte pluridisciplinaire **HAL**, est destinée au dépôt et à la diffusion de documents scientifiques de niveau recherche, publiés ou non, émanant des établissements d'enseignement et de recherche français ou étrangers, des laboratoires publics ou privés.



Distributed under a Creative Commons Attribution 4.0 International License



## Global 4DVAR Assimilation and Forecast Experiments Using AMSU Observations over Land. Part I: Impacts of Various Land Surface Emissivity Parameterizations

FATIMA KARBOU, ELISABETH GÉRARD, AND FLORENCE RABIER

*CNRM-GAME, Météo-France and CNRS, Toulouse, France*

(Manuscript received 9 December 2008, in final form 5 June 2009)

### ABSTRACT

To improve the assimilation of Advanced Microwave Sounding Unit-A and -B (AMSU-A and -B) observations over land, three methods, based either on an estimation of the land emissivity or the land skin temperature directly from satellite observations, have been developed. Some feasibility studies have been performed in the Météo-France assimilation system in order to choose the most appropriate method for the system. This study reports on three 2-month assimilation and forecast experiments that use different methods to estimate AMSU-A and -B land emissivities together with the operational run as a control experiment. The experiments and the control have been subjected to several comparisons. The performance of the observation operator for simulating window channel brightness temperatures has been studied. The study shows considerable improvements in the statistics of the window channels' first-guess departures (bias, standard deviation). The correlations between the observations and the model's simulations have also been improved, especially over snow-covered areas. The performances of the assimilation system, in terms of cost function change, have been examined: the cost function is generally improved during the screening and remains stable during the minimization. Moreover, comparisons have been made in terms of impacts on both analyses and forecasts.

### 1. Introduction

Microwave observations from the Advanced Microwave Sounding Unit-A and -B [AMSU-A and -B; or Microwave Humidity Sounder (MHS)] instruments have been widely used in numerical weather prediction (NWP) to improve the initial conditions for short-range forecasts. AMSU instruments are on board low-orbiting satellites such as the different generations of the National Oceanic and Atmospheric Administration (NOAA) satellites, the National Aeronautics and Space Administration's (NASA) *Aqua* mission, and more recently from the *MetOp-A* mission. Table 1 presents the general characteristics of the AMSU-A and -B channels and the conditions of their use within the four-dimensional variational data assimilation (4DVAR) system used in France. The list of conditions to be satisfied for a given channel (listed in Table 1) is not exhaustive. Many other conditions have to be satisfied to assimilate those ob-

servations. Observations from AMSU-A provide information about the temperature distribution in the atmosphere, thanks to 11 out of 15 channels, which are located near the oxygen absorption band (50–60 GHz). AMSU-B makes measurements at five frequencies; three of them are located near the strong water vapor line and are used to measure the humidity in the atmosphere. Besides their sounding capabilities, AMSU-A and -B have the so-called window channels, which give measurements that are sensitive to the surface and to low-level atmospheric layers (23.8, 31.4, 50.3, 89, and 150 GHz). Both instruments view the earth with a scan angle (zenith angle) that varies from  $-48^\circ$  ( $-58^\circ$ ) to  $+48^\circ$  ( $+58^\circ$ ) with respect to nadir.

Significant progress has already been achieved in the use of AMSU measurements in NWP, but in some areas the data remain underutilized. So far, priority was given to the use of AMSU measurements over seas, together with measurements for which the contribution of the surface is negligible. It should be pointed out that a classification-based emissivity scheme that uses regressions and empirical models (Weng et al. 2001; Grody 1988) has been used in NWP and has facilitated the assimilation of AMSU channels over land. The effectiveness

---

Corresponding author address: Fatima Karbou, CNRM-GAME, Météo-France and CNRS, 42 Av. Coriolis, 31057 Toulouse, France.  
E-mail: fatima.karbou@meteo.fr

TABLE 1. AMSU-A and -B characteristics and conditions for use.

Instrument	Channel	Frequency (GHz)	Sensitivity	Conditions for use	Obs (FG) errors
AMSU-A	1	23.8	Surface	Not used	—
	2	31.4	Surface	Not used	—
	3	50.3	Surface	Not used	—
	4	52.8	Temperature	Not used	—
	5	53.596 ± 0.115	Temperature	Used if open sea or land, and mean orography <500 m	0.45 (0.54)
	6	54.4	Temperature	Used if open sea, land, and mean orography <1500 m	0.35 (0.21)
	7	54.9	Temperature	Not used if cloudy,  lat  ≤ 30°	0.35 (0.17)
	8	55.5	Temperature	Not used if cloudy,  lat  ≤ 30°	0.35 (0.20)
	9	$\nu = 57.290$	Temperature	Used	0.35 (0.23)
	10	$\nu \pm 0.217$	Temperature	Used	0.35 (0.23)
	11	$\nu \pm 0.322 \pm 0.048$	Temperature	Used	0.50 (0.31)
	12	$\nu \pm 0.322 \pm 0.022$	Temperature	Used	0.80 (0.41)
	13	$\nu \pm 0.322 \pm 0.010$	Temperature	Used	1.2 (0.64)
	14	$\nu \pm 0.322 \pm 0.0045$	Temperature	Not used	—
	AMSU-B	15	89	Surface	Not used
1		89	Surface	Not used	—
2		150	Surface	Not used	—
3		183 ± 1	Humidity	Used if open sea, land, and mean orography <1500 m	3.00 (2.63)
4		183 ± 3	Humidity	Used if open sea, land, and mean orography <1000 m	2.50 (2.28)
	5	183 ± 7	Humidity	Used if open sea	2.00 (2.12)

of these models depends on the input parameters about the surface, for which a global analysis does not always exist. To date, observations are more intensively used over sea than over land thanks to effective sea emissivity models (Deblonde and English 2000; Guillou et al. 1998; Prigent and Abba 1990; Guissard and Sobieski 1987; Wentz 1975; Rosenkranz and Staelin 1972; Kazumori et al. 2008; Boukabara and Weng 2008; Ellison et al. 2003).

Unlike sea observations, the assimilation of land observations presents some persistent problems due to large errors while modeling the land surface (English 2007). The land surface emissivity at microwave frequencies is often close to 1.0 (over sea, it is always below 0.8 and often is as low as 0.5) and varies in a complex way at least with the surface conditions, roughness, and

moisture. Many studies have been carried out to improve our understanding of the land emissivity variability (Choudhury 1993; Felde and Pickle 1995; Jones and Vonder Haar 1997; Karbou et al. 2005; Morland et al. 2000, 2001; Prigent et al. 1997, 2000; Mätzler 1994; Ruston and Vonder Haar 2004; Ruston et al. 2008, among others), but only a few of them have addressed the issue of land emissivity modeling within the constraints of variational assimilation (Prigent et al. 2005; Karbou et al. 2006, 2007; O'Dell and Bauer 2007; Krzeminski et al. 2008; Ruston et al. 2008; Hilton et al. 2005). A review of the land surface emissivity modeling schemes used for data assimilation at many NWP centers is given in Karbou (2007).

This paper is a follow-on of Karbou et al. (2006) in which different strategies were proposed to describe the

TABLE 2. Description of three methods to describe the land surface emissivity ( $\epsilon$ ) and skin temperature ( $T_s$ ).

Method	AMSU-A	AMSU-B
1	$\epsilon$ : channel 3 emissivity from atlas (50 GHz) $\epsilon$ is given to temperature channels $T_s$ is from the short-range forecast	$\epsilon$ : channel 1 emissivity from atlas (89 GHz) $\epsilon$ is given to humidity channels $T_s$ is from the short-range forecast
2	$\epsilon$ : channel 3 retrieved emissivity $\epsilon$ is given to temperature channels $T_s$ is from the short-range forecast	$\epsilon$ : channel 1 retrieved emissivity $\epsilon$ is given to humidity channels $T_s$ is from the short-range forecast
3	$\epsilon$ : channel 3 emissivity from atlas $\epsilon$ is given to temperature channels $T_s$ is retrieved from channel 3	$\epsilon$ : channel 1 emissivity from atlas $\epsilon$ is given to humidity channels $T_s$ is retrieved from channel 1

TABLE 3. Overview of the assimilation experiments. Conditions for use of the AMSU observations are presented in Table 1.

Expt	Surface description	Used AMSU channels over land
CTL	Empirical models*	AMSU-A: channels 5–14 AMSU-B: channels 3 and 4
EXP1	Method 1	Same as in CTL
EXP2	Method 2	Same as in CTL
EXP3	Method 3	Same as in CTL

\* Empirical versions of Weng et al. (2001) and Grody et al. (1988).

land surface emissivity and/or the land skin temperature and to improve the assimilation of microwave measurements over land and within the constraints of a 4DVAR assimilation system. The treatment of the land surface, as proposed in Karbou et al. (2006), has been fully tested in this paper. Our purpose here is to examine the impacts of different land emissivity schemes, with no additional channels within the assimilation, in order to identify the most appropriate one to use with a 4DVAR assimilation system. Other assimilation experiments, using the land surface scheme identified as the most appropriate one, have been run to study the effects of assimilating land observations never assimilated before.

These experiments are studied in Karbou et al. (2010, hereafter Part II).

The global assimilation and forecast experiments are described in section 2 together with an overview of the land emissivity methods. The impacts on analyses and on forecasts are discussed in section 3. Results concerning the sensitivity of the analysis to land surface observations are also presented in section 3. Our conclusions are given in section 4.

## 2. The assimilation experiments

### a. The land surface emissivity modeling

As mentioned earlier, this paper relies on land emissivity developments, fully described in Karbou et al. (2006), and aims to improve the assimilation of AMSU-A and -B observations over land in the Météo-France 4DVAR system. If one wants to improve the description of the land surface emissivity in the model, it is essential to draw lessons from previous land emissivity analysis studies. In particular, the following assumptions have been adopted. For most surface types, land emissivity varies smoothly with frequency and for cross-track instruments, like AMSU-A and -B, emissivities retrieved

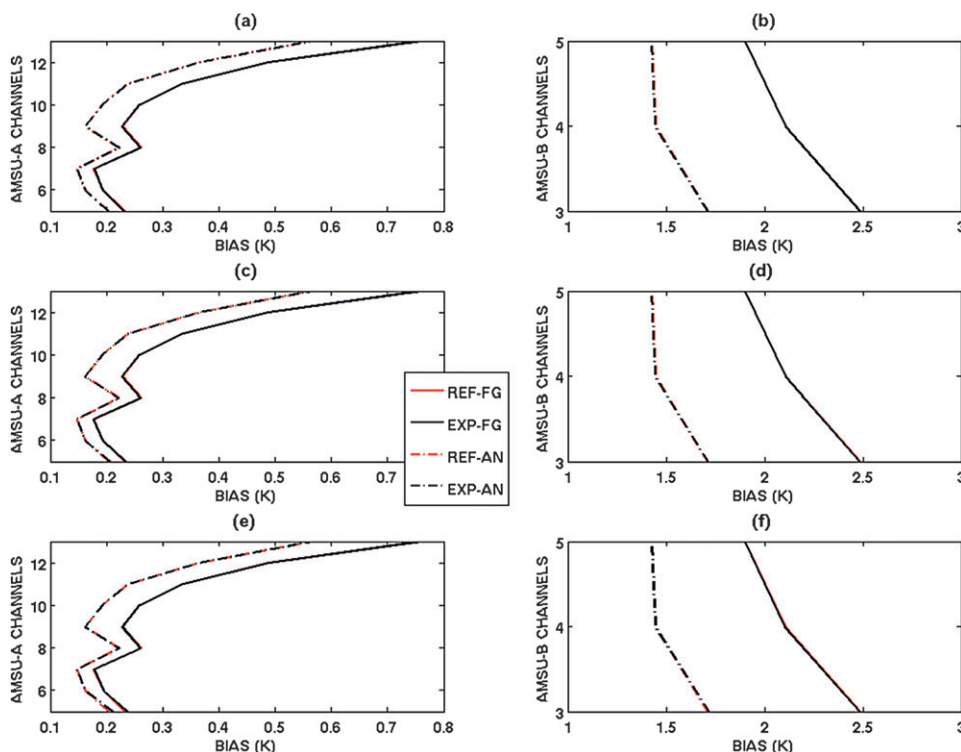


FIG. 1. Bias for the FG (solid) and the analysis departures (dashed) when using (a) AMSU-A and (b) AMSU-B observations for EXP1 (black) and CTL (red). Results are for the globe and for August 2006. (c),(d) As in (a),(b), respectively, but for the EXP2 results. (e),(f) As in (a),(b), respectively, but for the EXP3 results.

from “window” channels can be used as a “good approximation” for sounding channels. Therefore, three methods have been tested to check if the use of land emissivity and/or skin temperature directly calculated from satellite observations is relevant and if it improves the assimilation of surface-affected observations (Karbou et al. 2006). These highly complex methods have been interfaced with the RTTOV model (Eyre 1991; Saunders et al. 1999; Matricardi et al. 2004) and have been first applied to AMSU-A and -B measurements. In the following, we give a summary of the three land surface methods (see Table 2 as well):

- 1) For the first method (called method 1 hereafter), a 2-month emissivity climatology is used. The climatology gives mean values of the land emissivity at several AMSU window channels (23.8, 31.4, 50.3, and 89 GHz). Emissivities for sounding channels are taken from their estimates at the closest, in frequency, window channels. For instance, averaged emissivities at 50 GHz (AMSU-A channel 3) and at 89 GHz (AMSU-B channel 1) are assigned to AMSU-A temperature sounding channels and to AMSU-B humidity sounding channels, respectively. Our experiment using method 1 is called EXP1.
- 2) The second method (called method 2 hereafter) uses dynamically varying emissivities derived at each pixel using only one channel per instrument. The dynamically estimated emissivity is then assigned to the remaining channels without any frequency parameterization. Our experiment using method 2 is called EXP2.
- 3) Finally, the third method (called method 3 hereafter) combines the two previous approaches. This method uses averaged emissivities and a dynamically estimated skin temperature at each pixel using one window channel per instrument. The estimated skin temperature replaces the surface temperature originating from the model’s short-range forecasts. It is worth mentioning that the surface temperature in the Action de Recherche Petite Echelle Grande Echelle (ARPEGE) system is analyzed using an optimal interpolation method, which is applied on air temperature background information from the nearest level to the surface as well as on synoptic observations. Our experiment using method 3 is called EXP3.

Further details about land emissivity and skin temperature computations are given in Karbou et al. (2006).

#### *b. The assimilation system and the experiments*

This study is based on the Météo-France assimilation and forecast system (ARPEGE), which uses a 6-h time window and a multi-incremental 4DVAR scheme

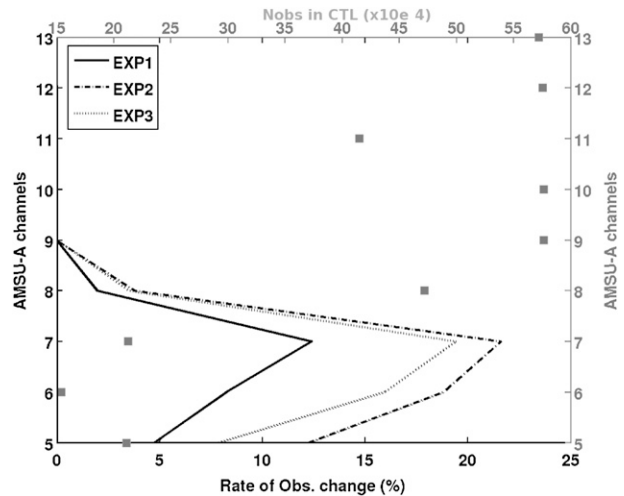


FIG. 2. Rates of increase or decrease for the numbers of assimilated observations over sea and land for EXP1–EXP3 with respect to CTL as a function of AMSU-A channels. For each experiment, the rate is calculated for all used AMSU-A observations as  $\text{Nobs}(\text{EXP}) - \text{Nobs}(\text{CTL})$  normalized by  $\text{Nobs}(\text{CTL})$ . The results are for August 2006; the total number of assimilated observations in CTL is also presented (gray-filled squares).

(Courtier et al. 1994; Veersé and Thépaut 1998; Rabier et al. 2000). The ARPEGE system was developed in collaboration with European Centre for Medium-Range Weather Forecasts (ECMWF). The assimilation system seeks a state of the atmosphere that represents the optimal balance between observations and the background information (short-range forecast from a previous analysis). The 2-month assimilation experiments have been run using the ARPEGE system in its July 2006 operational version. The assimilation system has a 6-hourly cycle at T358 spectral truncation on a stretched sphere with a stretching factor of 2.4 and 46 vertical levels (from 17 m to 45 km). This configuration leads to a horizontal resolution that varies from 23 km over Europe to 135 km over the antipodes. The operational assimilation system uses a wide range of conventional observations (surface stations, buoys, upper-air measurements, radiosondes) and satellite observations (atmospheric motion vectors from geostationary satellites, radiances from polar-orbiting satellites). For satellite data, ARPEGE uses an adaptive variational bias correction method, which is applied to reduce biases between satellite observations and their model equivalent (Auligné et al. 2007).

A set of four 2-month assimilation and forecast experiments is analyzed in this paper. The list of all assimilation experiments is given in Table 3. One of these experiments represents the assimilation system in its July 2006 operational version and provides the control assimilation used as a reference in this study. Another set of three 2-month assimilation experiments has been

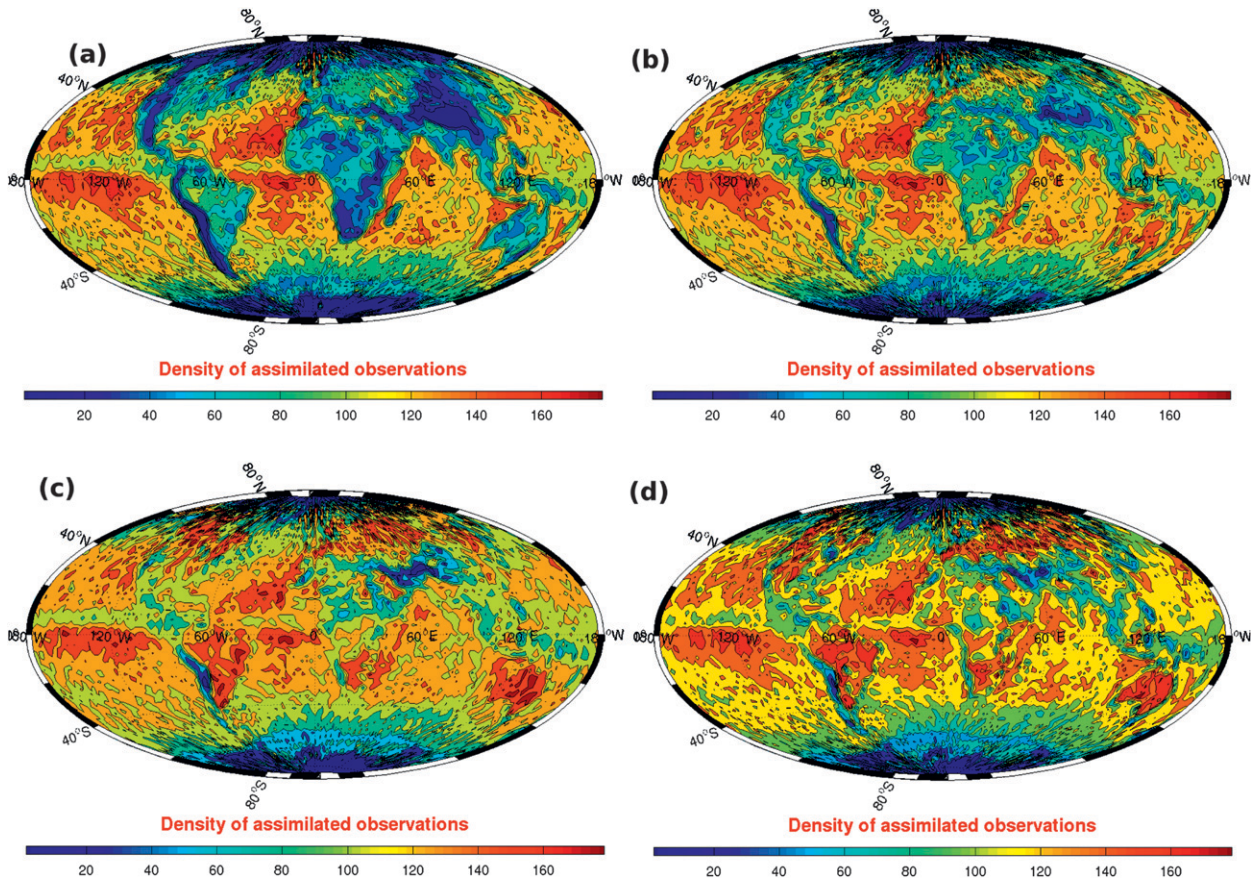


FIG. 3. Map of the density of the assimilated observations from AMSU-A channel 7. The density values have been computed by counting the number of assimilated observations falling in a grid cell of  $2^{\circ} \times 2^{\circ}$  during 45 days (1 Aug–14 Sep 2006). Results are for (a) CTL, (b) EXP1, (c) EXP2, and (d) EXP3.

separately studied in Part II. The two sets of experiments have been separated for two reasons: (a) to examine the impacts of different land emissivity schemes without adding any other channels in order to identify the most appropriate choice for the ARPEGE system and then (b) to use the selected land surface scheme to study the effects of assimilating observations that have never been assimilated previously.

Experiment CTL is our control experiment and is representative of the operational ARPEGE system. Experiments EXP1, EXP2, and EXP3 only differ from the CTL by the methods used to determine the land surface emissivity and/or the skin temperature. In July 2006, the Météo-France 4DVAR system used empirical versions of Grody (1988) or Weng et al. (2001) models to obtain emissivity estimates at AMSU frequencies. EXP1 is identical to CTL except that the land emissivities for AMSU-A and -B are taken from a land emissivity climatology. EXP2 is also identical to CTL except that the land emissivities for the AMSU observations are dynamically estimated using a selection of surface channels. Regarding EXP3, the land

surface emissivity has been determined using an emissivity climatology, and the land skin temperature has been dynamically estimated at selected AMSU surface channels (see section 2a for more details about the emissivity methods). The experiments have produced global analyses four times per day and 4-day forecasts every day at 0000 UTC. For all the experiments, the initial conditions were taken from the operational analysis at 1800 UTC on 14 July 2006. The first 2 weeks of the runs have been excluded for an optimal set up of the experiments, excluding a warm-up phase in our diagnostics. Unless specified differently, all comparisons and diagnostics will be made using run outputs from 1 August to 14 September 2006.

### 3. Results

#### *a. On the analysis and first-guess fit to the assimilated observations*

For all three of our experiments, the model fit to assimilated observations, except for AMSU, has been found to

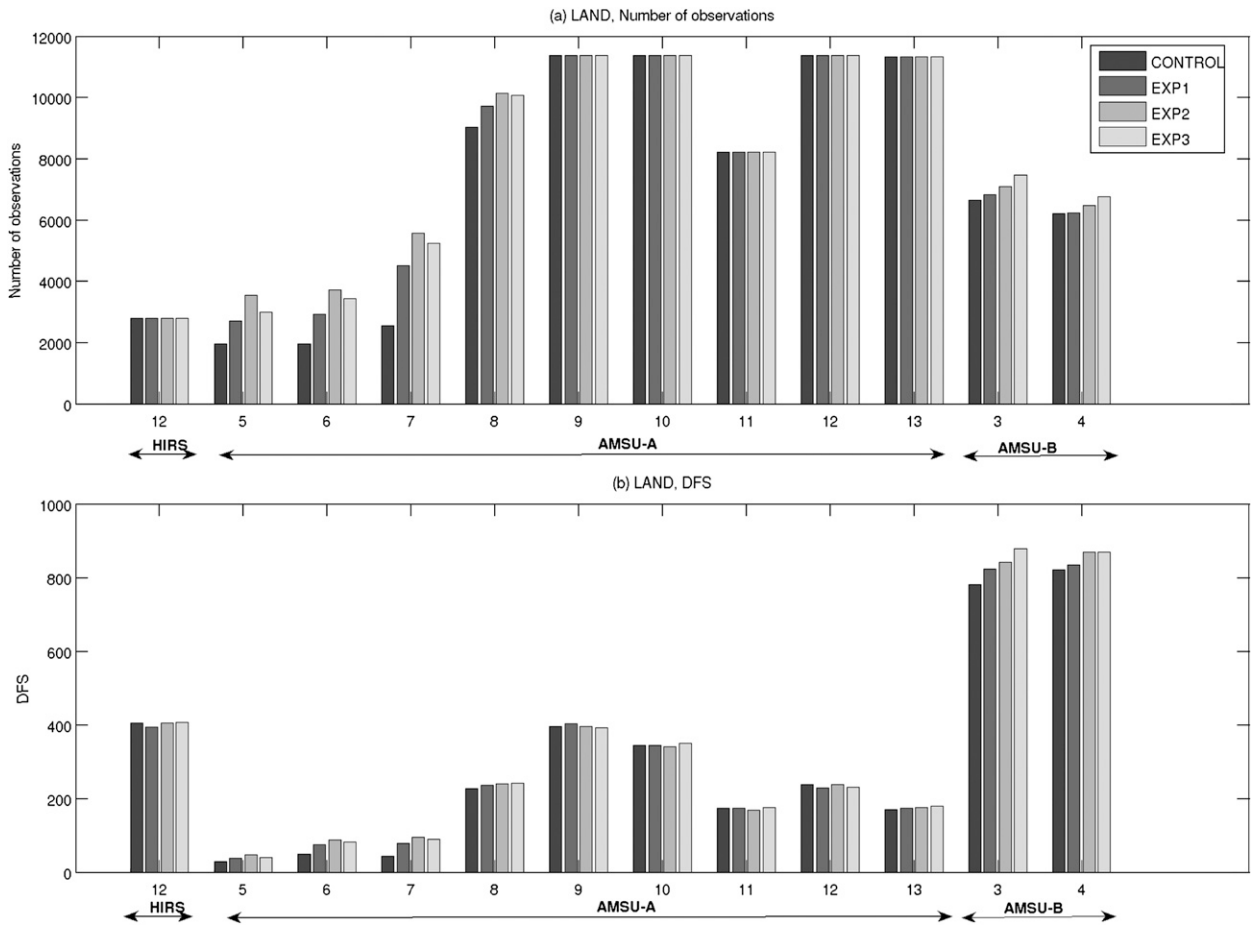


FIG. 4. (a) Number of assimilated observations over land and (b) their DFS values per observation types.

perform as well as in CTL. The fits of the AMSU observations compared to the first guesses (FGs) or the analysis have been improved, taking into account the large amount of added data over land. Figure 1 shows the bias (in K) for the FGs (solid) and the analysis departures (dashed) for the assimilated AMSU-A and -B observations in CTL (red) and in our three other experiments (black). The results are from August 2006 and are given for EXP1 (Fig. 1a for AMSU-A and Fig. 1b for AMSU-B), for EXP2 (Fig. 1c for AMSU-A and Fig. 1d for AMSU-B), and for EXP3 (Fig. 1e for AMSU-A and Fig. 1f for AMSU-B). Figure 2 shows the corresponding increase or decrease, with respect to CTL, of the total number of AMSU-A observations as a function of AMSU-A channels for EXP1–EXP3. The total number of observations per channel in CTL is also presented. As mentioned earlier, one should note that no degradation of the fit of the model to the observations can be seen even if a significant additional amount of data has been assimilated (see Fig. 2). When considering the total number of observations (sea and land), increases of about 12%, 22%,

and 19% have been noted for AMSU-A channel 7 for EXP1–EXP3, respectively. However, when considering land observations only, the increases for channel 7 are close to 75%, 130%, and 120% for EXP1–EXP3, respectively (not shown). More geographic details about the increase in the number of assimilated AMSU-A channel 7 observations are given in Figs. 3a–d. Figure 3 shows mean density maps of AMSU-A observations, which have been assimilated during August 2006 in CTL and EXP1–EXP3, respectively. One should notice that the CTL density map can be used as a land–sea mask since land surfaces can clearly be distinguished on this map. When the density of assimilated observations is taken into account, it is more difficult to make out land from sea surfaces for EXP2 and EXP3. For these last two experiments, the assimilation of AMSU-A channel 7 seems to be more homogeneous over all surfaces.

As mentioned earlier, more microwave observations are assimilated in EXP1–EXP3 with respect to CTL. What remains to be determined is how the analysis has responded to additional land observations.

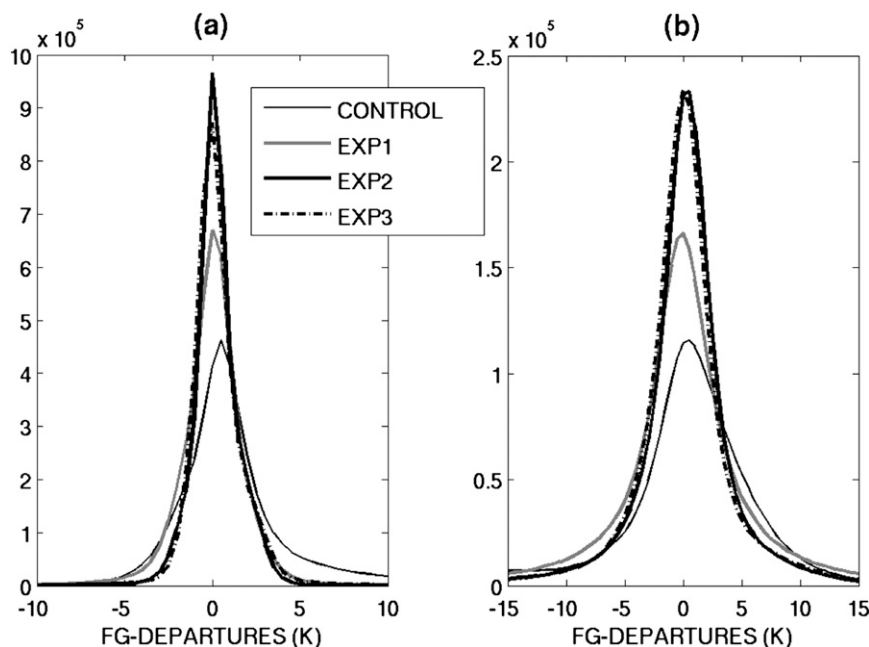


FIG. 5. Histograms of FG departures (observations minus first guess without bias correction) obtained over land and for (a) AMSU-A channel 4 and (b) AMSU-B channel 2. Results from the control experiment and EXP1–EXP3 are shown.

To address this issue, the degrees of freedom for signal (DFSs) diagnostics have been used. These diagnostics are believed to give some insights into the relative impacts of each observation type on the analysis. Following the method introduced by Desroziers and Ivanov (2003) and used by Chapnik et al. (2006), the DFSs have been approximated given an analysis of the state of the atmosphere, a background state, and a set of random perturbations of the observation vector. To calculate the DFS, two parallel analyses are run: an original analysis of the atmosphere and its associated perturbed analysis using perturbed observations. For such a computation, several analyses are necessary to reduce the uncertainty of the analysis variance reduction. In this paper, the DFS has been calculated using four global analyses for 2 August 2006 at 0, 6, 12, and 18 h. For each original analysis, 16 perturbed analyses have been computed. We end up with 16 estimations of the DFS per cycle. Then, an averaged DFS is calculated and will be analyzed in the following.

Figure 4 shows the number of observations and their DFSs for satellite observations assimilated over land. As pointed out earlier, one should note the significant increase in the number of assimilated observations at sounding channels for all three experiments. The number of observations from channels 5–7 has increased by more than 90% in EXP2. The rate of increase is also important for EXP1 and EXP3. The increase in the

number of assimilated observations is associated with an increase in the observation DFS. For instance, the number of observations from channel 7 has increased by about 120% in EXP3 and their DFSs by about 110%. Similar conclusions can be drawn for AMSU-B channels even if the increase in the number of observations is smaller than for AMSU-A observations. This means that the analysis has responded to the newly assimilated observations over land. For AMSU-A, the best results are obtained with EXP2, whereas for AMSU-B they are best with EXP3. At this stage, it is worth mentioning that the DFS estimate should be carefully interpreted since it depends, among other parameters, on the structure function associated with the background error, on the ratio between observation and background errors, and also on the density of observations. Moreover, the DFS is a linear estimation of impact and cannot be used to infer the impacts of observations that are involved with stronger nonlinearity mechanisms such as humidity observations. To conclude for this section, the land emissivity methods have been found to be helpful in increasing the number of assimilated temperature and humidity sounding observations over land. Such a data increase has been made possible with the advent of reliable descriptions of the surface (emissivity and/or surface temperature), which improve the performance levels of the observation operator at window channels and increase the number of observations that pass the

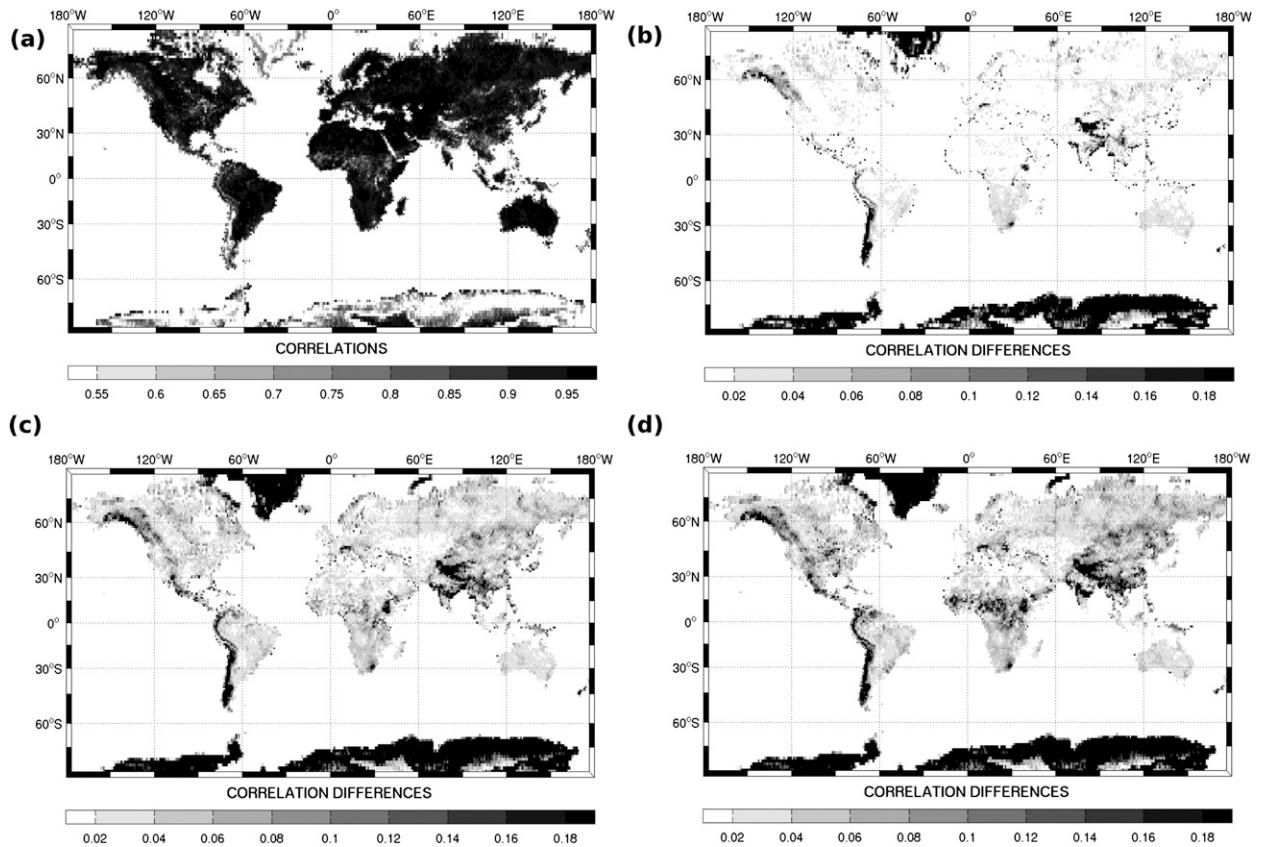


FIG. 6. (a) Map of the correlations between observations and simulations of AMSU-A channel4 in CTL. The correlation values have been computed using data falling in a grid cell of  $1^\circ \times 1^\circ$  size during the first 2 weeks of August 2006. Map of the correlation differences: (b) EXP1 – CTL, (c) EXP2 – CTL, and (d) EXP3 – CTL.

quality control tests (noted as QC tests hereafter). The QC test issue will be further discussed in the following section.

*b. Insights into the performance of the observation operator for window channels and into the cost function change*

The assimilation of temperature and humidity observations depends on many conditions; one of them is a quality control test using FG departures from AMSU-A channel 4 (noted AMA4 hereafter) and AMSU-B channel 2 (noted AMB2 hereafter) to reject data with too strong cloud contamination. AMB2 FG departures should be within  $\pm 5$  K and AMA4 FG departures should be within  $\pm 0.7$  K. Moreover, the surface temperature should be greater than 278 K (for AMSU-B) and some other conditions of orography are also required for the assimilation of AMSU-A and -B channels (see Table 1 for the conditions for the use of AMSU measurements). Consequently, improving AMA4 and AMB2 FG departures is very important for the assimilation of sounding channels. For instance, if a QC test fails for one AMB2

pixel, then all AMSU-B pixels for the same location are rejected.

So far, many observations are incorrectly rejected because values for the land surface emissivity or of skin temperature are inappropriate. The two window channels receive an important contribution from the surface and are very sensitive to the land surface emissivity. Figure 5 shows histograms of FG departures (observations minus first guesses) obtained globally over land for AMA4 (Fig. 5a) and for AMB2 (Fig. 5b). Results are for CTL and EXP1–EXP3 with no bias correction. For all three experiments, window channel FG-departure statistics compare favorably with CTL. The improvements are very large for EXP2 and EXP3, which partly reflects the otherwise insufficient specification of the surface emissivities in CTL. The FG departures are further studied by analyzing the correlations between the window channel observations and the simulated model brightness temperatures (Tbs). In Fig. 6a (Fig. 7a), a map of the mean correlations between the AMA4 (AMB2) observations and their Tbs simulations from CTL is presented. The correlations have been computed for each

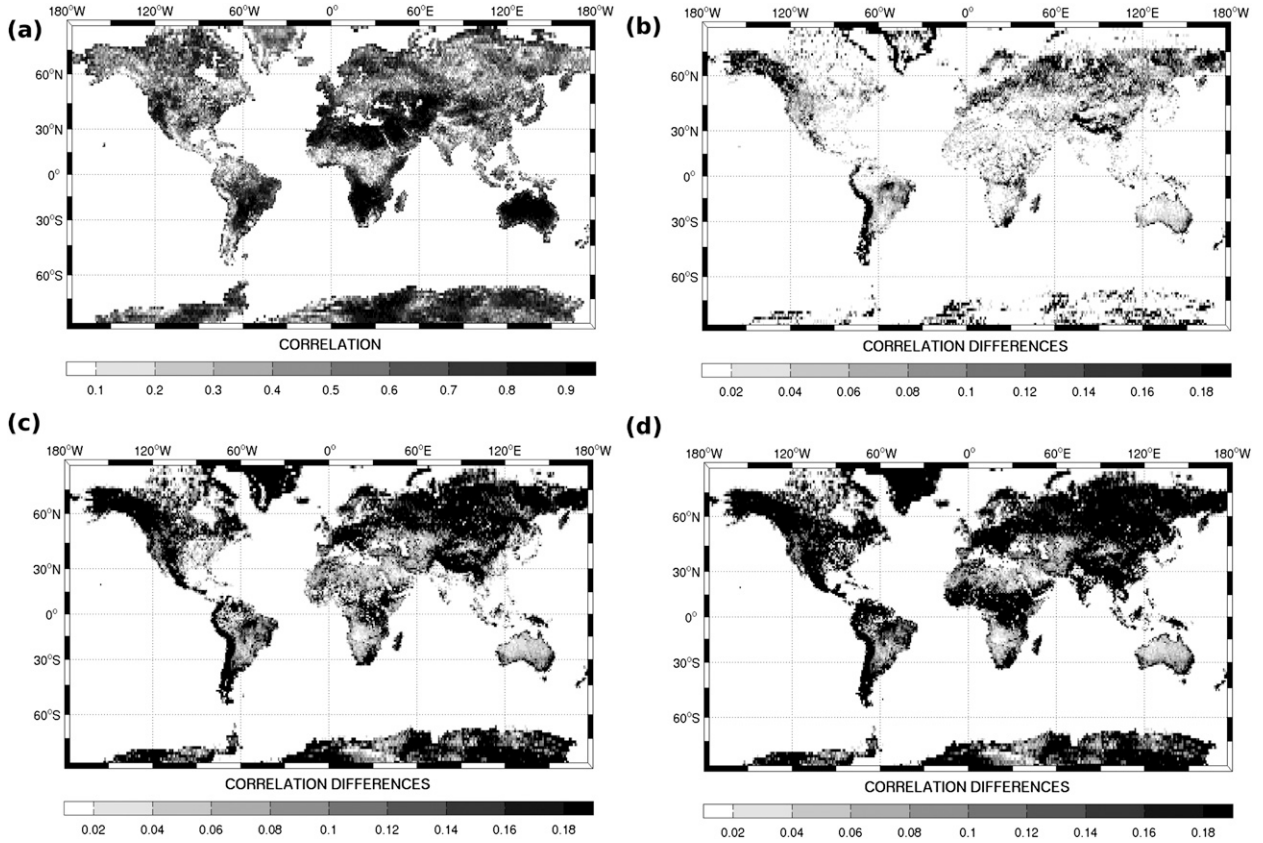


FIG. 7. As in Fig. 6, but for correlations between the observations and simulations of AMSU-B channel 2.

$1^\circ \times 1^\circ$  grid cell using data from the first two weeks of August 2006. The mean AMSU correlation maps are presented together with maps of the differences in the correlations between CTL and the three other experiments (Fig. 6b for EXP1 minus CTL, Fig. 6c for EXP2 minus CTL, and Fig. 6d for EXP3 minus CTL). For AMA4, the correlations have been improved for all three experiments with respect to CTL. The correlation change varies with surface type and is maximal over snow areas (more than 20% of the improvement in the correlations). The best results are obtained with EXP2 and EXP3 with a mean improvement of 20%–5% from the high latitudes to the tropics. Regarding the AMB2 results, one may notice the large improvement in the correlations between the observations and the simulations in EXP2 and EXP3. The best results are obtained in EXP3 with an improvement to the correlations of about 20% over many areas. EXP3 appears to be very promising as it provides better model equivalents to AMA4 and AMB2 over land. However, more in-depth studies are still needed before advocating this method. Further tests will deal with some surface temperature evaluation against independent measurements; they will also study possible emissivity error propagation into

surface temperature estimates and consider ways to adjust the land emissivity during assimilation (by including it in the control variable for instance).

As stated earlier, the improvement of the AMA4 and AMB2 FG departures directly impacts the QC tests within the 4DVAR and can also impact the overall behavior of the system. In data assimilation, a 4DVAR system finds the model solution that represents the optimal balance between all of the available information (observations and background information). If one assumes that the observations and background errors are uncorrelated and have Gaussian distributions, then the 4DVAR solution  $\mathbf{x}$  (state of the atmosphere) is obtained by minimizing a cost function  $J(\mathbf{x})$  given by

$$J(\mathbf{x}) = \frac{1}{2}(\mathbf{x} - \mathbf{x}^b)^T \mathbf{B}^{-1}(\mathbf{x} - \mathbf{x}^b) + \frac{1}{2} \sum_{i=0}^N [\mathcal{H}_i(\mathbf{x}_i) - \mathbf{y}_i^o]^T \mathbf{R}_i^{-1} [\mathcal{H}_i(\mathbf{x}_i) - \mathbf{y}_i^o], \quad (1)$$

where  $\mathbf{x}$  is the model state at time  $t_0$ ,  $\mathbf{x}^b$  is the background state at time  $t_0$ ,  $\mathbf{B}$  is the background error covariance

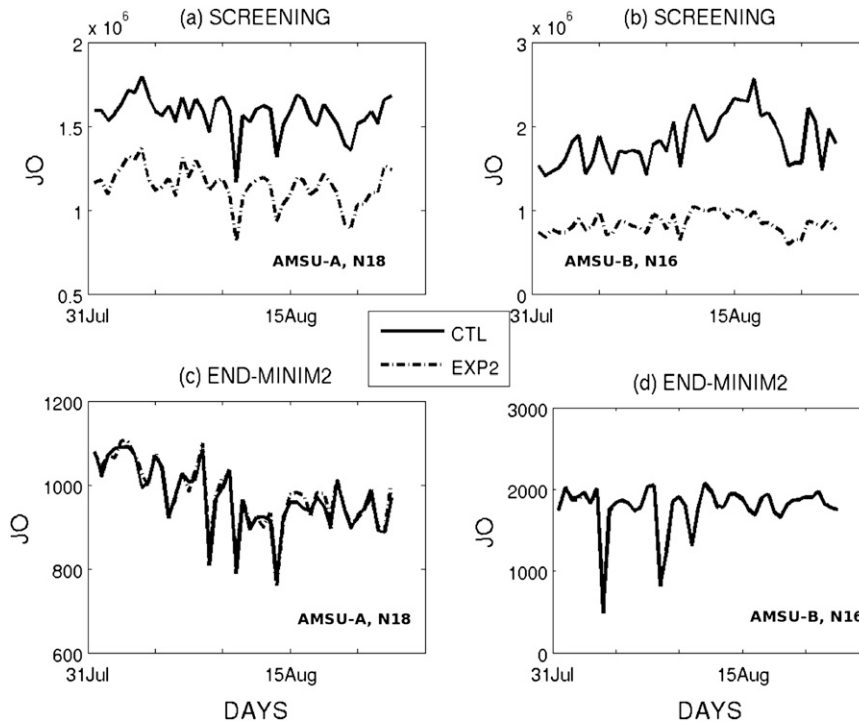


FIG. 8. Time series of JO changes during the screening process in CTL (solid line) and in EXP2 (dashed line) for (a) AMSU-A NOAA-18 data and for (b) NOAA-16 AMSU-B data. (c),(d) As in (a),(b), but at the end of the second minimization.

matrix of  $\mathbf{x}^b$ ,  $\mathbf{y}_i^o$  is the observation vector at time  $t_i$ ,  $\mathcal{H}_i$  is the observation model operator at time  $t_i$ ,  $\mathbf{R}_i$  is the observation error covariance matrix at time  $t_i$  (including  $\mathcal{H}_i$  errors),  $\mathbf{x}_i$  is the model state at time  $t_i$ , and superscripts  $-1$  and T indicate the matrix inverse and transpose, respectively.

In ARPEGE, the minimization of Eq. (1) is performed in two steps: with simplified and with more complete physics, respectively (Janiskova et al. 1999). To check the effects of the QC tests on the system, the cost function results (called JO hereafter) have been examined: 1) during the screening step (computation of a model's equivalents using FG fields) and 2) at the end of the second minimization. Figure 8 shows daily time series of the JO change during the screening step and at the end the second minimization in CTL (solid lines) and in EXP2 (dashed lines) for AMSU-A and -B data from NOAA-18 and -16, respectively. JO during the screening step is calculated using all available observations whereas JO at the end of the second minimization is computed using assimilated data in the system. Figure 9 is similar to Fig. 8 but displays JO/N results ( $N$  is the number of observations). Overall, the EXP2 performances are better than those of CTL: AMSU JOs are systematically and significantly reduced during the screening. One should note here that the number of in-

put AMSU observations in CTL is identical to the one in EXP2. During the screening process, the EXP2 JO (or JO/N) has been improved by about 27% for AMSU-A and by 54% for AMSU-B with respect to CTL. At the end of the second minimization, the EXP2 JO for AMSU is similar to the CTL JO. This means that the change in land surface emissivity helps improve the performances of the QC tests without damaging the system during assimilation. When considering all observations, the JO improvement in EXP2 with respect to CTL is close to 7% during the screening and is negligible at the end of the second minimization (see Fig. 10). Results from EXP1 and EXP3 are comparable with those of EXP2 (not shown).

### c. The forecast impacts

The forecast performances of CTL and EXP1–EXP3 have been compared by examining the short-range verification scores of precipitation (24 h) and the longer-range verification scores (up to 4 days) for the mass, wind, relative humidity, and temperature fields. For long-range verification scores, the forecast root-mean-square errors (RMSEs) for each field have been calculated for August 2006 and for all three experiments, with the radiosonde observations being the target estimations. The relative impact on each parameter has been evaluated by

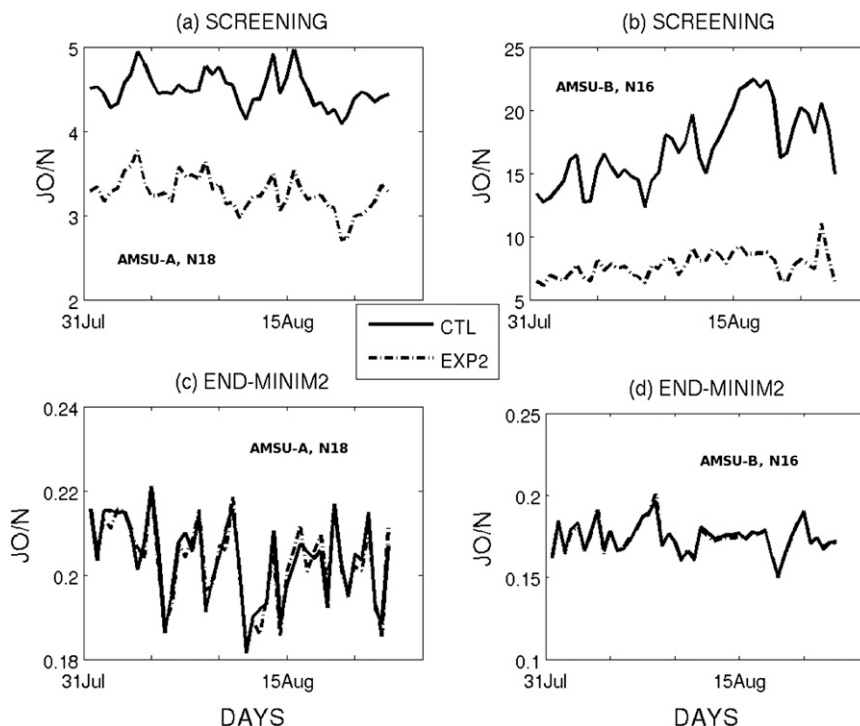


FIG. 9. As in Fig. 8, but for JO/N, where  $N$  is the number of observations.

computing the normalized relative increase or decrease in the forecast RMSE with respect to the CTL experiment  $[(\text{RMSE}(\text{CTL}) - \text{RMSE}(\text{experiment}))/\text{RMSE}(\text{CTL})]$ . The general findings about the forecast verification results are that no major impact has been noticed in any of the domains (Northern and Southern Hemispheres, tropics). Note that the forecasts in ARPEGE are limited to day 4. Studies in Karbou et al. (2007) have shown a positive impact on the geopotential height (500 hPa) in the Southern Hemisphere for a forecast range beyond 5 days when using the land emissivity method 2 for AMSU-A and for AMSU-B (experiment equivalent to EXP2). The forecast improvements have been found to be significant at the 90% confidence level or better.

The forecast impacts have also been studied in terms of short-range forecasts of precipitation. Figure 11 shows the total 24-h precipitation differences as provided by CTL (Fig. 11a), EXP1 – CTL (Fig. 11b), EXP2 – CTL (Fig. 11c), and EXP3 – CTL (Fig. 11d). The assimilation of more microwave observations from sounding channels slightly increases the rainfall over the tropics for all three experiments. The increase seems to be larger for EXP3 over land. This could be explained by the fact that EXP3 assimilates more AMSU-B observations than does EXP2. For comparison purposes, it is useful to have an insight into the change of the analysis of the total column water vapor (TCWV). Figure 12b shows the mean analysis dif-

ference in TCWV between EXP1 and CTL averaged over 45 days (1 August–14 September 2006). When the TCWV differences are positive (negative), EXP1 is more moist (dry) than CTL. Figure 12c shows results for EXP2 – CTL and Fig. 12d results are for EXP3 – CTL. The main change in TCWV has been observed in the tropics for all three experiments. EXP3 (and to a lesser extent EXP2) seems to emphasize atmospheric moistening over Mauritania and Mali. The atmospheric moistening not only concerns the surface but also many levels of the atmosphere (up to 700 hPa).

#### 4. Discussion

Several global assimilation and forecast experiments have been run in order to identify the most appropriate land surface scheme for the assimilation of AMSU measurements in the ARPEGE system. Three methods for estimating the land surface emissivity and/or the skin temperature have been previously developed as part of the Météo-France assimilation system (Karbou et al. 2006) and have been further studied in this paper. The first method (method 1) uses a land surface emissivity climatology. For the second method (method 2), the land surface emissivity is dynamically calculated for selected surface channels, for each pixel and for each

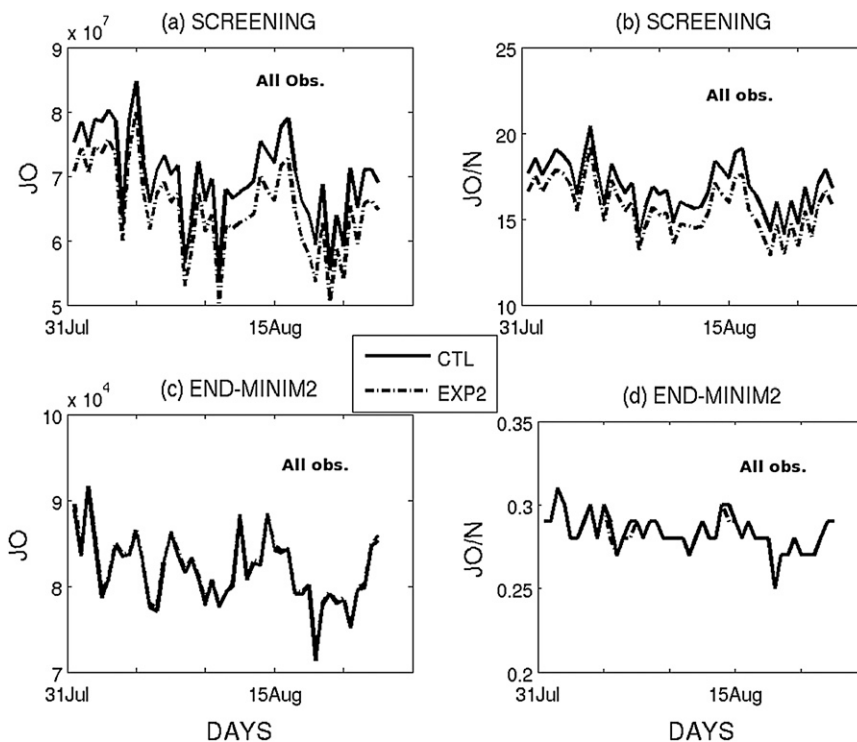


FIG. 10. Time series of (a) JO and (b) JO/ $N$  changes during the screening in CTL (solid line) and in EXP2 (dashed line) for all observations, with  $N$  being the number of observations. (c), (d) As in (a), (b), but at the end of the second minimization.

atmospheric situation. The third method (method 3) combines methods 1 and 2 with the estimation of the skin temperature at selected surface channels and for each atmospheric situation. The impacts of using different land surface emissivity schemes (methods 1–3) have been studied with respect to a control experiment that was representative of the operational model. The comparison has been made by looking into the performance levels of the observation operator over land for assimilated channels and unused window channels. It has been found that the use of an updated land emissivity scheme is very helpful in reducing both the bias and standard deviation of FG departures from window channels (AMSU-A channel 4 and AMSU-B channel 2). The best results have been obtained with experiments using methods 2 and 3. These two methods increase the correlations between the observations and simulations of the window channels. The improvement is very large over snow-covered areas. Regarding the assimilated data, we have noticed an important increase in the amount of assimilated AMSU observations over land when using one of the three land emissivity methods. The increase in the number of assimilated observations does not degrade the global statistics of the departures from the first guess and from analysis. The performance

levels of the assimilation system during the screening step and during the minimization have been examined: the cost function is generally improved during the screening and remains stable during the minimization. The impacts of the three land emissivity methods have also been studied in terms of their forecast impacts. The impacts on forecast have been found to be neutral for all domains. The general findings about the land surface method comparison indicate that methods 2 and 3 are the most promising. Method 3 has a great deal of potential since it combines the estimation of the land surface emissivity (using an atlas) and the estimation of the land surface temperature. At this stage, it is desirable to further evaluate method 3 to validate the skin temperature estimations at microwave frequencies. Further studies focusing on method 3 are already planned. As mentioned above, method 2 has been found to be very useful in improving the assimilation of AMSU-A and -B observations over land. This method is further evaluated in Part II, where several assimilation experiments that assimilate, for the first time ever, low-level microwave observations over land, have been run. Finally, let us point out that the Météo-France assimilation system has been using method 2 operationally for land emissivity estimations at AMSU-A and at AMSU-B frequencies since

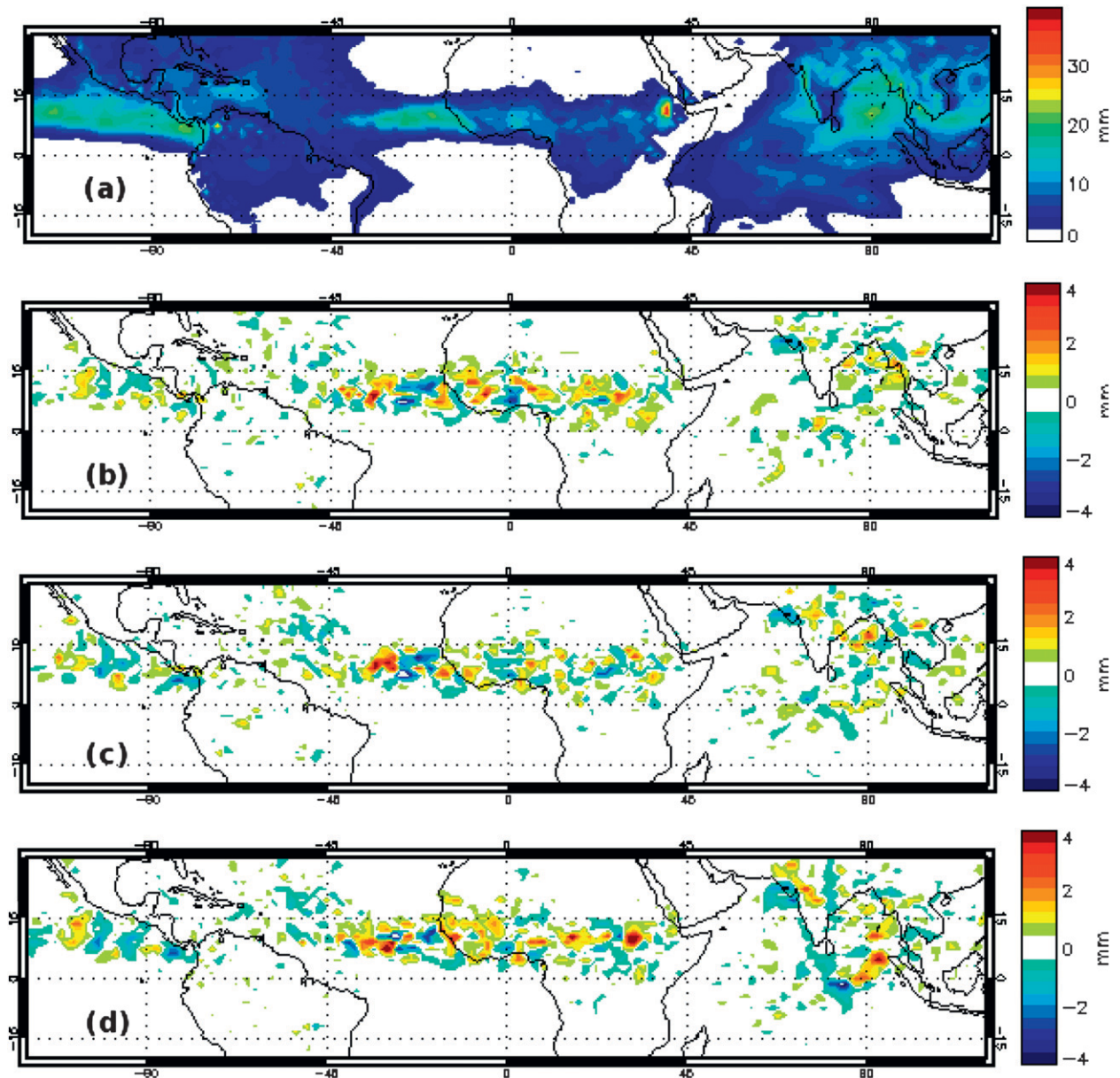


FIG. 11. Average of the 24-h cumulated rain rate over 45 days (1 Aug–14 Sep 2006) showing (a) CTL and (b) EXP1 – CTL. Positive (negative) values indicate that EXP1 has increased (decreased) precipitations. (c) As in (b), but for EXP2. (d) As in (b), but for EXP3.

July 2008. In connection with this work, an important land surface emissivity database has been developed at the Centre National de Recherches Météorologiques/ Groupe d'études de l'atmosphère météorologique (CNRM/GAME). This emissivity database contains an averaged land surface emissivity climatology and models (data for 2005–09) from many microwave instruments, including AMSU-A and -B. These data, available for use by the scientific community, may be found online (<http://www.cnrm.meteo.fr/gmap/mwemis/mwemis.html>).

*Acknowledgments.* The authors would like to deeply thank three anonymous reviewers for their numerous constructive insights; their suggestions greatly improved the manuscripts. The authors wish to thank Jean Maziejewski for his help in revising the manuscript. The authors would like to thank Bernard Chapnik, Paul Poli, Gerald Desroziers, and Joel Stein for their help with the DFS computation and interpretation. The authors wish to thank Alan Geer for his help with the IDL routines.

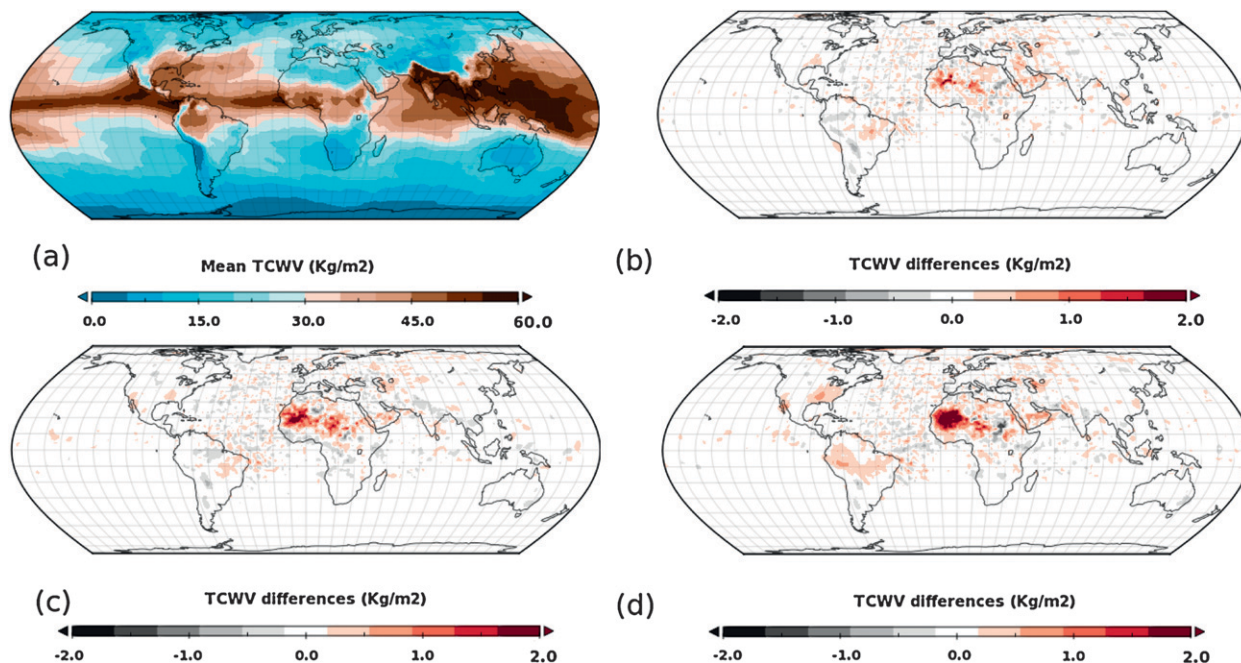


FIG. 12. (a) Mean analysis for TCWV for the CTL and (b) mean TCWV analysis difference for EXP1 with respect to the control experiment. Statistics have been derived using 45 days (1 Aug–14 Sep 2006). Negative (positive) values indicate that the control assimilation is moister (dry) than the EXP1 experiment. (c) As in (b), but for EXP2. (d) As in (b), but for EXP3.

#### REFERENCES

- Auigné, T., A. P. McNally, and D. P. Dee, 2007: Adaptive bias correction for satellite data in a numerical weather prediction system. *Quart. J. Roy. Meteor. Soc.*, **133**, 631–642.
- Boukabara, S.-A., and F. Weng, 2008: Microwave emissivity over ocean in all weather conditions: Validation using WindSat and airborne GPS dropsondes. *IEEE Trans. Geosci. Remote Sens.*, **46**, 393–402.
- Chapnik, B., G. Desroziers, F. Rabier, and O. Talagrand, 2006: Diagnosis and tuning of observational error in a quasi-operational data assimilation. *Quart. J. Roy. Meteor. Soc.*, **132**, 543–565.
- Choudhury, B. J., 1993: Reflectivities of selected land surface types at 19 and 37 GHz from SSM/I observations. *Remote Sens. Environ.*, **46**, 1–17.
- Courtier, P., J. N. Thépaut, and A. Hollingsworth, 1994: A strategy for operational implementation of 4D-Var using an incremental approach. *Quart. J. Roy. Meteor. Soc.*, **120**, 1367–1387.
- Deblonde, G., and S. English, 2000: Evaluation of FASTEM and FASTEM2 fast microwave oceanic surface emissivity model. *Proc. 11th Int. ATOVS Study Conf.*, Budapest, Hungary, WMO, 67–78.
- Desroziers, G., and S. Ivanov, 2003: Diagnosis and adaptive tuning of information error parameters in a variational assimilation. *Quart. J. Roy. Meteor. Soc.*, **129**, 1433–1452.
- Ellison, W. J., and Coauthors, 2003: A comparison of ocean emissivity models using the Advanced Microwave Sounding Unit, the Special Sensor Microwave Imager, the TRMM Microwave Imager, and airborne radiometer observations. *J. Geophys. Res.*, **108**, 4663, doi:10.1029/2002JD003213.
- English, S., 2007: The importance of accurate skin temperature in assimilating radiances from satellite sounding instruments. *IEEE Trans. Geosci. Remote Sens.*, **46**, 403–408.
- Eyre, J., 1991: A fast radiative transfer model for satellite sounding systems. ECMWF Tech. Memo. 176, 28 pp. [Available from ECMWF, Shinfield Park, Reading RG2 9AX, United Kingdom.]
- Felde, G. W., and J. D. Pickle, 1995: Retrieval of 91 and 150 GHz earth surface emissivities. *J. Geophys. Res.*, **100**, 20 855–20 866.
- Grody, N. C., 1988: Surface identification using satellite microwave radiometers. *IEEE Trans. Geosci. Remote Sens.*, **26**, 850–859.
- Guillou, C., W. Ellison, L. Eymard, K. Lamkaoui, C. Prigent, G. Delbos, G. Balana, and S. A. Boukabara, 1998: Impact of new permittivity measurements on sea surface emissivity modelling in microwaves. *Radio Sci.*, **33**, 649–667.
- Guisard, A., and P. Sobieski, 1987: An approximate model for the microwave brightness temperature of the sea. *Int. J. Remote Sens.*, **8**, 1607–1627.
- Hilton, F., S. English, and C. Paulsen, 2005: Establishing a microwave land surface emissivity scheme in the Met Office 1D-Var. *Proc. 14th Int. ATOVS Study Conf.*, Beijing, China, 559.
- Janiskova, M., J. N. Thépaut, and J. F. Geleyn, 1999: Simplified and regular physical parameterization for incremental four dimensional variational assimilation. *Mon. Wea. Rev.*, **127**, 26–44.
- Jones, A. S., and T. H. Vonder Haar, 1997: Retrieval of microwave surface emittance over land using coincident microwave and infrared satellite measurements. *J. Geophys. Res.*, **102** (D12), 13 609–13 626.
- Karbou, F., 2007: Treatment of surface emissivity in satellite data assimilation. *Proc. Seminar on Recent Developments in the Use of Satellite Observations in Numerical Weather Prediction*, Reading, United Kingdom, ECMWF, 167–185.
- , C. Prigent, L. Eymard, and J. Pardo, 2005: Microwave land emissivity calculations using AMSU-A and AMSU-B measurements. *IEEE Trans. Geosci. Remote Sens.*, **43**, 948–959.

- , E. Gérard, and F. Rabier, 2006: Microwave land emissivity and skin temperature for AMSU-A and -B assimilation over land. *Quart. J. Roy. Meteor. Soc.*, **132**, 2333–2355.
- , N. Bormann, and J.-N. Thépaut, 2007: Towards the assimilation of satellite microwave observations over land: Feasibility studies using SSM/Is, AMSU-A and AMSU-B. Rep. NWPSAF-EC-VS-010, 37 pp.
- , F. Rabier, J.-P. Lafore, J.-L. Redelsperger, and O. Bock, 2010: Global 4DVAR assimilation and forecast experiments using AMSU observations over land. Part II: Impacts of assimilating surface-sensitive channels on the African monsoon during AMMA. *Wea. Forecasting*, **25**, 20–36.
- Kazumori, M., Q. Liu, R. Treadon, and J. C. Derber, 2008: Impact study of AMSR-E radiances in the NCEP Global Data Assimilation System. *Mon. Wea. Rev.*, **136**, 541–559.
- Krzeminski, B., N. Bormann, F. Karbou, and P. Bauer, 2008: Towards a better use of AMSU over land at ECMWF. *Proc. 16th Int. TOVS Study Conference*, Angra dos Reis, Brazil, WMO, 157–165. [Available online at [http://cimss.ssec.wisc.edu/itwg/itsc/itsc16/report/ITSC\\_16\\_Proceedings.pdf](http://cimss.ssec.wisc.edu/itwg/itsc/itsc16/report/ITSC_16_Proceedings.pdf).]
- Matricardi, M., F. Chevallier, G. Kelly, and J. Thépaut, 2004: Channel selection method for IASI radiances. *Quart. J. Roy. Meteor. Soc.*, **130**, 153–173.
- Mätzler, C., 1994: Passive microwave signatures of landscapes in winter. *Meteor. Atmos. Phys.*, **54**, 241–260.
- Morland, J., I. David, F. Grimes, G. Dugdale, and T. J. Hewison, 2000: The estimation of land surface emissivities at 24 GHz to 157 GHz using remotely sensed aircraft data. *Remote Sens. Environ.*, **73**, 3323–3336.
- , —, —, and T. J. Hewison, 2001: Satellite observations of the microwave emissivity of a semi-arid land surface. *Remote Sens. Environ.*, **77**, 2149–2164.
- O'Dell, C., and P. Bauer, 2007: Assimilation of precipitation-affected SSM/I radiances over land in the ECMWF data assimilation system. SAF-Hydrology Rep. PR-VS31, 51 pp.
- Prigent, C., and P. Abba, 1990: Sea surface equivalent brightness temperature at millimeter wavelength. *Ann. Geophys.*, **8**, 627–634.
- , W. B. Rossow, and E. Matthews, 1997: Microwave land surface emissivities estimated from SSM/I observations. *J. Geophys. Res.*, **102**, 21 867–21 890.
- , J. Wigneron, B. Rossow, and J. R. Pardo, 2000: Frequency and angular variations of land surface microwave emissivities: Can we estimate SSM/T and AMSU emissivities from SSM/I emissivities? *IEEE Trans. Geosci. Remote Sens.*, **38**, 2373–2386.
- , F. Chevallier, F. Karbou, P. Bauer, and G. Kelly, 2005: AMSU-A surface emissivities for numerical weather prediction assimilation schemes. *J. Appl. Meteor.*, **44**, 416–426.
- Rabier, F., H. Jarvinen, E. Klinker, J. F. Mahfouf, and A. Simmons, 2000: The ECMWF operational implementation of four-dimensional variational assimilation. I: Experimental results with simplified physics. *Quart. J. Roy. Meteor. Soc.*, **126**, 1143–1170.
- Rosenkranz, P. W., and D. Staelin, 1972: Microwave emissivity of ocean foam and its effect on nadir radiometric measurements. *J. Geophys. Res.*, **77**, 6528–6538.
- Ruston, B. C., and T. H. Vonder Haar, 2004: Characterization of summertime microwave emissivities from the Special Sensor Microwave Imager over the conterminous United States. *J. Geophys. Res.*, **109**, D19103, doi:10.1029/2004JD004890.
- , F. Weng, and B. Yan, 2008: Use of one-dimensional variational retrieval to diagnose estimates of infrared and microwave surface emissivity over land for ATOVS sounding instruments. *IEEE Trans. Geosci. Remote Sens.*, **46**, 376–384.
- Saunders, R. W., M. Matricardi, and P. Brunel, 1999: An improved fast radiative transfer model for assimilation of satellite radiance observations. *Quart. J. Roy. Meteor. Soc.*, **125**, 1407–1425.
- Veersé, F., and J. N. Thépaut, 1998: Multiple truncation incremental approach for four-dimensional variational data assimilation. *Quart. J. Roy. Meteor. Soc.*, **124**, 1889–1908.
- Weng, F., B. Yan, and N. Grody, 2001: A microwave land emissivity model. *J. Geophys. Res.*, **106**, 20 115–20 123.
- Wentz, F., 1975: A two scale scattering model for foam-free sea microwave brightness temperatures. *J. Geophys. Res.*, **80**, 3441–3446.